Experimental study of ripple dimensions under steady current

Ellynn Bouvet[a] *University of Le Havre Normandy, France – ellynn.bouvet@doct.univ-lehavre.fr*
Armelle Jarno[a] *University of Le Havre Normandy, France – jarnoa@univ-lehavre.fr*
Olivier Blanpain *SHOM, Brest, France – olivier.blanpain@shom.fr*
Thierry Garlan *SHOM, Brest, France – Thierry.garlan@shom.fr*
François Marin[a] *University of Le Havre Normandy, France – francois.marin@univ-leahvre.fr*
[a]*Laboratoire Ondes et Milieux Complexes, UMR 6294 CNRS*

ABSTRACT: Sand ripples have been the subject of many studies. Numerous empirical formulas exist to describe their dimensions. In this paper, ripple height and length are studied at equilibrium state in a current flume. The impact of the grain size and grain shape are analysed. This work is the first stage to estimate ripple characteristics induced by a current, under simple configurations.

1. INTRODUCTION

Ripples are often formed when the shear stress generated by the hydrodynamics is high enough for sediments to be set in motion. They are ubiquitous in coastal seas and river, their dimensions have been widely studied in the past years: e.g. Baas (1994), Baas (2009) and Zhang (2009) studied the morphology of ripples in a laboratory flume. Boguchwal & Southard (1989) and Doucette (2002) studied ripples in their natural environment. The complexity of the subject makes it the subject of many recent studies. Numerous parameters are involved and have an impact on the motion of grains which can depends on the medium grain diameter or grain shape.

Natural environments are extremely complex and ripples are generally formed by a wide range of grain size or an unstable current. Over the years, dimensions of current induced ripples have been widely studied (e.g. Yalin 1977, Flemming 2000, Zhang et al. 2009, Soulsby 2012, Perillo 2014). They suggest that the medium grain size D_{50} has a key role on the ripple morphology and propose an empirical model to estimate ripple height and length. The most common formula used is (Yalin 1964):

$$\lambda = 1000\, D_{50} \quad (1)$$

$$\eta = 0.08\, \lambda^{0.95} \quad (2)$$

Based on Baas (1994) expressions, Soulsby (2012) proposed a revisited empirical model that fits better with his data set:

For $1.2 < D_* < 16$

$$\eta = D_{50}\, 202\, D_*^{-0.554} \quad (3)$$

$$\lambda = D_{50}(500 + 1881\, D_*^{-1.5}) \quad (4)$$

Where $D_* = D_{50}\left[\frac{g(s-1)}{\nu^2}\right]^{1/3}$, g is the gravitational acceleration $(m.s^{-2})$, s is specific density of sand and ν the kinematic viscosity $(m^2.s^{-1})$. Zhang (2009) carried out an experimental study with natural sands and suggests that the characteristic height and length depends on the grain size Reynolds number $(Re_* = \frac{u_* D_{50}}{\nu})$:

$$\frac{\lambda}{D_{50}} = 191.76\, Re_*^{0.3} \quad (5)$$

$$\frac{\eta}{D_{50}} = 1.97\, Re_*^{1.3} \quad (6)$$

The objective of this study is to describe the dimensions of bedforms generated by a unidirectional flow in a laboratory flume. The use of a flume allows the control of a few parameters: the medium grain size, the current speed and a constant depth. Ripple dimensions are measured once the equilibrium time is reached. In the present article, the aim is to quantify the impact of grain size on ripples and therefore, two sands are tested: a very fine sand and a medium sand. Furthermore, the impact of the grain shape is studied as well with the use of a third sand composed of shells debris. The impact of current speed on bedforms morphology is also tested on each sand.

2. EXPERIMENTAL SETUP

2.1 The flume

Experiments are conducted in the current flume of the University of Le Havre Normandy. It is 10 m long, 0.49 m wide and 0.49 m deep with glass walls (Figure 1). The current is generated with the help of a pump that recirculates the water in a closed circuit. A honeycomb is fixed at the entrance of the channel to break up large-scale turbulent structures in the flow.

Sediments are introduced into the flume and lay above an artificial bottom. A particular attention is paid on the flatness of the initial sediment bed. Transported particles fall into sediment traps located at the end of the flume, allowing the measurement of bedload transport. A smooth slope is imposed right after the honeycomb so that sediments are not eroded early on and jeopardise the measurements.

1. 2.2 Tests conditions

In order to point out the influence of the particle size and shape on bedforms, three natural sands are tested. One is a very fine sand with a D_{50} of $119\ \mu m$ and two others have similar sized: one has a D_{50} of $356\ \mu m$ and is fully constituted of silica grains while the other has a D_{50} of 381 µm and contains 39% of carbonate debris. Tests were performed with acid etching to quantify the percentage of carbonate debris. These debris are marine shattered shell and have a flatten shape which distinguish them from silica particles that have a shape more rounded. The three sands are considered well sorted (in accordance with the standard deviation of Soulsby (2012), $\sigma_g = \sqrt{D_{84}/D_{16}}$). Their characteristics are summarized in Table 1.

Tests were realized with three currents speed: $0.33, 0.40$ and 0.47 m s^{-1}. The water depth was set to 25 cm and the thickness of the bed to 7 cm so that all the experiments are performed with an infinite sediment supply. In accordance with Boguchwal & Southard (1989), all the test conditions are made so that the type of bedforms generated in the flume are ripples (Figure 2).

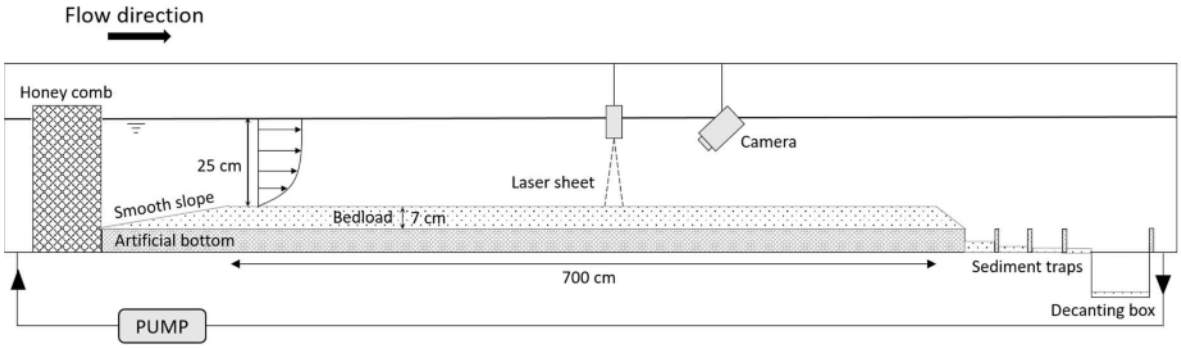

Figure 1. The current flume of the University of Le Havre Normandy

Table 1. Characterization of sands

	Fine	Medium Sand	Medium shell sand
D_{50} (μm)	119	356	381
σ_g^2	1.29	2.04	2.98
Shell debris (%)	<1%	<1%	39%

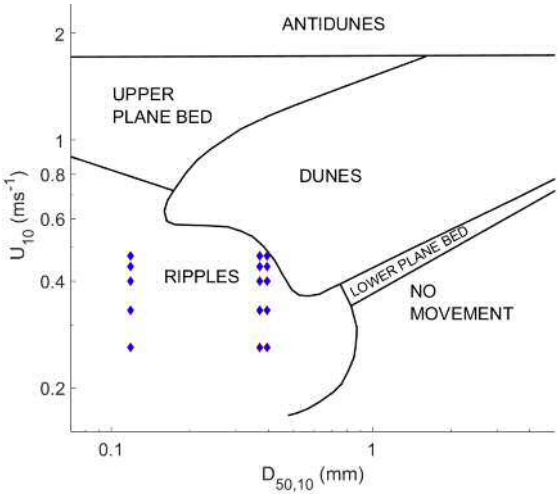

Figure 2. Plot of mean flow velocity against sediment size showing stability fields of bed phases (Modified from Boguchwal & Southward 1989).

2.3 Methods

A special care was paid to the experimental protocol (especially with the initial flat bed). The current is slowly increased to avoid an early erosion of the bottom. It takes 300 seconds for the current to reach its full speed. The test lasts until the ripples field is well established (the wavelength and ripple height are frequently monitored until they reach a statistically constant state). Afterwards, the current is stopped. The bathymetry is then acquired using a camera settled on a moving rail above the flume (Fig. 1). The camera records the deformation of a laser sheet projected on the bottom and they both move along the flume and covers about 3 meters of bathymetry. Finally, the full bathymetry is rebuilt in 3D with post-processing methods using MATLAB Software. Ripple heights are measured from one trough to the next crest. The wavelength considered is the total distance between two troughs (Zhang 2009).

3. RESULTS

Ripples fields equilibrium state is reached 9 to 17 hours after the beginning of the test depending on the sand: the fine sand reaches the equilibrium conditions more quickly than the two medium-sized sands.

Table 2 summarizes the results of the tests: the three current speeds are named V1, V2, V3 which corresponds respectively to the speeds $0.33, 0.4$ and 0.47 m.s^{-1}. A double value indicates the first and the second mode of the distribution. Height and wavelength are given in centimeters.

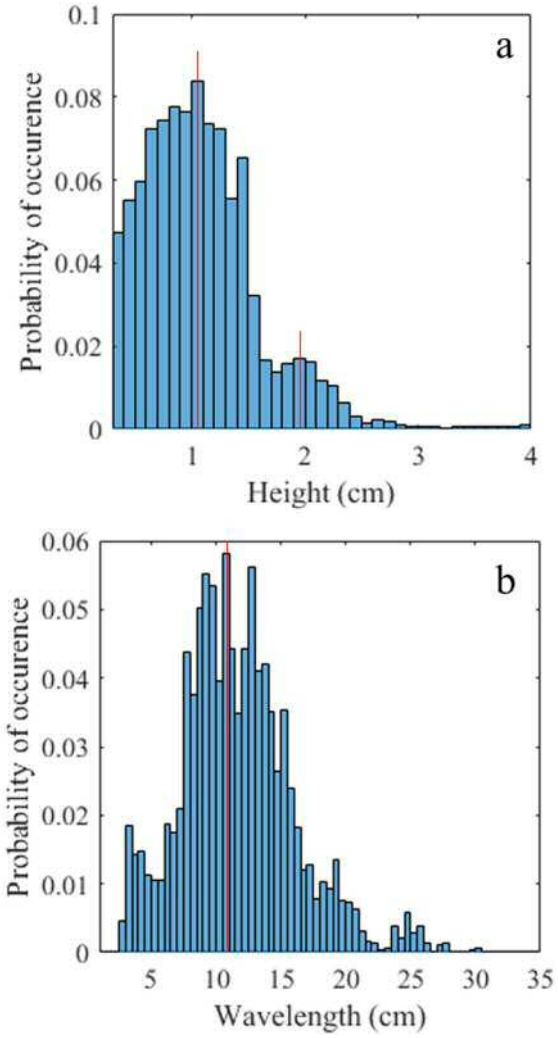

Figure 3. Height (a) and wavelength (b) distribution of the fine sand under low current speed (0.33 m.s^{-1}). The red lines indicate the most probable values.

Table 2. Bedform dimensions (cm)

Fine sand	V1	V2	V3
H_{mean}	0.96 / 2.16	0.8 / 2.04	0.99 / 2.13
H_{mode}	1.0 / 1.9	0.5 / 1.7	1.1 / 2
H_{max}	2.8	3.3	2.7
L_{mean}	11.7	13.4	14.1
L_{mode}	10.5	12.8	12
L_{max}	25.5	26	27
Medium sand	V1	V2	V3
H_{mean}	0.47 / 1.43	0.84 / 2.08	1.11 / 2.84
H_{mode}	0.4 / 1.4	0.4 / 2	0.4 / 2.75
H_{max}	3.2	2.9	3.7
L_{mean}	16	19.8	23.2
L_{mode}	12.5	18.5	24
L_{max}	31.5	37.5	44
Shell sand	V1	V2	V3
H_{mean}	1.18 / 2.46	1.48 / 3.2	1.27 / 2.94
H_{mode}	0.7 / 2.25	0.35 / 3.15	0.5 / 3.15
H_{max}	2.9	3.5	3.3
L_{mean}	17.7	23.6	25
L_{mode}	17	25.5	22
L_{max}	35	45	43

Table 3. Height and wavelength theoretical values

Height (cm)	Fine sand	Medium sand	Shell sand
Yalin (1964)	1.1	3.0	3.2
Soulsby (2002)	13.	2.1	2.2
Zhang (2009) V1	1.4	2.3	2.8
Zhang (2009) V2	2.4	3.8	4.6
Zhang (2009) V3	3.5	5.9	7.1

Wavelength (cm)	Fine sand	Medium sand	Shell sand
Yalin (1964)	11.9	35.6	38.1
Soulsby (2002)	10.2	20	21.4
Zhang (2009) V1	6	26	28.6
Zhang (2009) V2	6.6	29	32
Zhang (2009) V3	7.3	32.3	36

Results show that the height distribution for the three sands are multimodal. This means that ripple height can be regrouped and associated with several probable values. Figure 3 is an example of a height distribution that has two distinct modes and a wavelengths distribution that has one mode. Similar results were observed by Baas (1999). The probability of occurrence for a small ripple is higher than for a large one. It is illustrated in Figure 4: there is only a few numbers of large ripples and a majority of small ripples. The results analysis showed that the more the current speed increases the more the height distribution spreads: heights tend to shift towards medium heights. For each test distribution, the mean and the maximum values are calculated: the maximum is determined by averaging the upper 10% values. Maximum heights are constant.

The same analysis is performed on wavelength: mean wavelength slightly increases with the current and distributions have one distinct probable value. At equilibrium time, the dimensions of a ripple continue to be influenced by the current: vortices set the sediments in motion and erode large ripples. Their height and wavelength are lightly decreased. Eroded sediments create a new ripple with very small height and wavelength witch will itself slowly grow into a large ripple. Figure 5a demonstrates a cross-section of a standard large ripple that developed during the test with the shell sand at a medium speed: it has a wavelength of 23 cm and is 2.6 cm high. An hour later (Figure 5b), its height decreased to 1.8 cm and the lee has changed: a

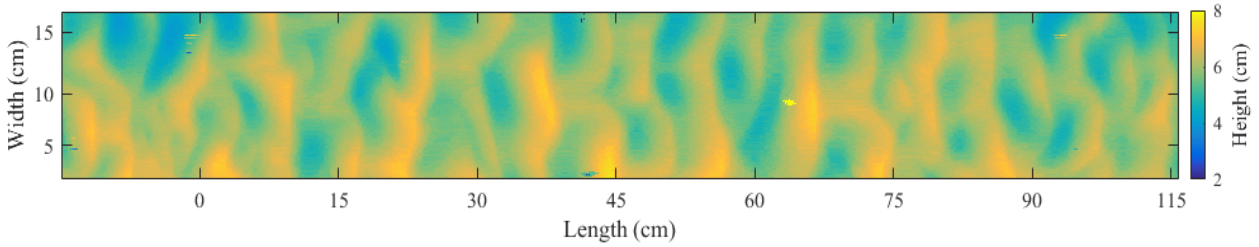

Figure 4. Bathymetry with the fine sand under low current speed $(0.33\ m.s^{-1})$.

deposition of sediment occurred. On Figure 5c a new ripple is created due to the sediment deposition. It is 0.4 cm high and 5.1 cm long and match with the first height mode of the test.

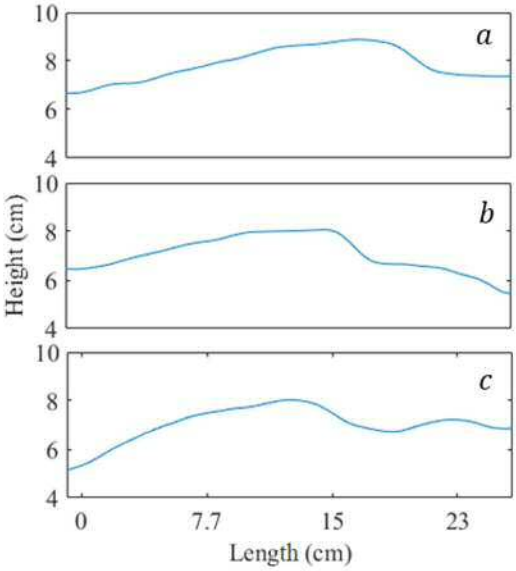

Figure 5. An example of a ripple development with the shell sand with a 0.4 $m.s^{-1}$ flow. a: At equilibrium state t = 0, b: crest has been eroded t = +1h, c: a new ripple was created t = +2h.

Table 3 summarizes theoretical values of height and wavelength from Yalin (1964), Soulsby (2002) and Zhang (2009) models.

Because of the distribution spreading, a correlation between height of this study and theoretical heights in literature is complex. However, Zhang (2009) found that the grain size Reynolds number can be taken into account to characterize the height and length of ripples. Wavelengths estimated from Equation 5 have same trends as these study wavelengths.

In the early stage of this study, no noticeable difference was observed between medium silica sand and shell sand.

3. CONCLUSION AND DISCUSSION

Results show that height and wavelength distributions are complex because of the wide range of bedforms dimensions. A ripple is continuously altered by the current thus vortices can relocate sediments downstream and create a new small ripple. Bedforms dimensions found in this study are nevertheless consistent with previous studies. Height and wavelength differences between medium silica sand and shell sand are not apparent. To take the analysis one step further, a statistical review will be performed. For instance, the use of the Principal Component Analysis (PCA) might bring new correlations to light.

Further studies will be carried out to investigate the impact of the sand heterogeneity on the bedforms: the very fine sand will be mixed with the medium sands (silica sand and carbonates debris).

In addition, the impact of bedforms on transport (both bedload and suspension) will be studied, each sand individually as well as the mixed sands.

Finally, results will be compared to simulations from a numerical model develop by the SHOM: HYCOM SEDIM.

4. ACKNOWLEDGEMENT

This research is part of a Ph. D. project. The authors would like to thanks Région Normandie and the DGA for founding this research project.

5. REFERENCES

Baas, J. A., 1999. An empirical model for the development and equilibrium morphology current ripples in fine sand. Sedimentology 46, 123-138.

Baas, J. H., 1994. A flume study on the development and equilibrium morphology of current ripples in very fine sand. Sedimentology 41, 185-209.

Boguchwal L. A., Southard. J., 1989. Bed configurations in steady unidirectional water flows. Part I. Scale model study using fine sands.

Doucette, J., 2002. Geometry and grain-size sorting of ripples on low-energy sandy beaches: field observations and model predictions. Sedimentology 49, 483-503.

Flemming, B. W., 2000. Marine sandwave dynamics. University of Lille, France: ISBN 2-11-088263-8.

Perillo M.M., Best. J., 2014. A unified model for bedform development and equilibrium under unidirectional, oscillatory and combined-flows. Sedimentology 61, 2063-2085.

Soulsby R. L., Whitehouse R. J., 2012. Prediction of time-evolving sand ripples in shelf seas. Continental Shelf Reasearch 38, 47-62.

Soulsby, R. L., 1997. Dynamics of marine sands. Springfield: Thomas Telford.

Yalin, M. S., 1964. Geometrical properties of sand waves. Journal of Hydraulics Div v90, 105-119.